ORIGINAL ARTICLE

Anti-adhesive effect of naturally obtained dicalcium phosphate dihydrate nanoparticles in the rat uterine wound model

Efecto antiadhesivo de nanopartículas de dihidrato de fosfato dicálcico obtenidas naturalmente en el modelo de herida uterina de rata

Begum Kurt[1], Kerim E. Oksuz[2], Zeynep D. Sahin-Inan[3], and Ceylan Hepokur[4]*

[1]Department of Obstetrics and Gynecology, Faculty of Medicine, Sivas Cumhuriyet University; [2]Department of Metallurgical and Materials Engineering, Sivas Cumhuriyet University; [3]Department of Histology and Embryology, Faculty of Medicine, Sivas Cumhuriyet University; [4]Department of Biochemistry, Faculty of Pharmacy, Sivas Cumhuriyet University. Sivas, Turkey

Abstract

Objective: *In this study, we aimed to compare the anti-adhesive effects of contractubex and dicalcium phosphate dihydrate (DCPD) particles in rats treated with the uterine horn adhesion model.* **Materials and methods:** *Newly adult, 60 Wistar albino rats were used as experimental animals. The modified rat uterine horn adhesion model was used to induce intra-abdominal adhesion. Tumor necrosis factor (TNF)-α, interleukin (IL)-1, vascular endothelial growth factor (VEGF) and transforming growth factor (TGF)-β1 were studied for biochemical and immunohistochemical examination.* **Results:** *TNF-α decreased in each group, while it decreased more in G2 and G3 than in G1. IL-1β decreased in each group, while it decreased the most in G3. TGF-β1 and VEGF localization was less in the G2 compared to G1, the least TGF-β1 and VEGF immunolocalization was detected in the G3 and G4. For both antibodies, the least localization among all groups belonged to G3. From day 7 to day 21, the highest TGF-β1 immunolocalization was observed in G1, lesser localization in G2 and lowest in G3.* **Conclusion:** *DCPD nanoparticles show promise as a clinical antiadhesive agent and should be further evaluated in experimental animal models and human trials.*

Keywords: *Dicalcium phosphate dihydrate. Gynecologic surgery. Nanoparticles. Wistar rats.*

Resumen

Objetivo: *En este estudio, nuestro objetivo fue comparar los efectos antiadhesivos de las partículas de contractubex (CTX) y fosfato dicálcico dihidratado (DCPD) en ratas tratadas con el modelo de adhesión del cuerno uterino.* **Materiales y métodos:** *Como animales de experimentación se utilizaron 60 ratas Wistar albinas, recién adultas. Se usó el modelo de adhesión del cuerno uterino de rata modificado para inducir la adhesión intraabdominal. Se estudiaron TNF-α, IL-1, VEGF y TGF-β1 para examen bioquímico e inmunohistoquímico.* **Resultados:** *el TNF-α disminuyó en cada grupo, mientras que disminuyó más en G2 y G3 que en G1. IL-1β disminuyó en cada grupo, mientras que disminuyó más en G3. La localización de TGF-β1 y VEGF fue menor en G2 en comparación con G1, la menor inmunolocalización de TGF-β1 y VEGF se detectó en G3 y G4. Para ambos anticuerpos, la localización mínima entre todos los grupos pertenecía a G3. Desde el día 7 hasta el día 21, la mayor inmunolocalización de TGF-β1 se observó en G1, menor localización en G2 y menor en G3.* **Conclusión:** *las nanopartículas de DCPD se muestran prometedoras como agentes antiadhesivos clínicos y deben evaluarse más en modelos animales experimentales y ensayos en humanos.*

***Palabras clave*:** *Fosfato dicálcico dihidratado. Cirugía ginecológica. Nanopartículas. Ratas Wistar.*

***Correspondence:**
Begum Kurt
E-mail: begumkurt@cumhuriyet.edu.tr

Date of reception: 24-02-2023
Date of acceptance: 15-04-2023
DOI: 10.24875/CIRU.23000097

Cir Cir. 2023;91(4):457-467
Contents available at PubMed
www.cirugiaycirujanos.com

Introduction

Adhesions are the results of the inflammatory response to tissue trauma, infection, bleeding, or foreign matter in the peritoneal space[1-3]. There are many studies on the development of barrier materials, hormones and their agonists/antagonists, hyaluronic acid, fibrinolytic agents, nonsteroidal anti-inflammatory drugs, and antioxidants to prevent postoperative adhesion formation[4,5]. The vast majority of them could not enter surgical practice, and a significant part could not gain applicability in our surgical technique because of the high cost[3,4,6].

CTX gel (Merz Pharma GmbH and Co., Frankfurt, Germany) is applicated to reduce inflammation and fibroblast proliferation that occurs in the early stages of wound healing[7,8]. Studies have shown that CTX application causes a decrease in the immunoreactivity of transforming growth factor-β (TGF-β), laminin, and fibronectin. It has been shown in previous studies that there is no adhesion, toxic effect or granuloma when applied intra-abdominal[9]. Due to its known antioxidant, anti-inflammatory, and fibroblast-inhibiting effects, it reduces histopathological damage scores when applied to extracutaneous tissues[10].

DCPD nanopowders calcium phosphate, orthophosphates (PO43-), metaphosphates or pyrophosphates (P2O74-), and especially hydrogen or hydroxide ions together with calcium ions are mineral groups. In animal and clinical experiments, it has been observed that the in-vivo solubility of biocompatible tissue-healing biomaterials with DCPD as the main phase after crystallization and curing or containing DCPD particles is high. It is completely dissolved in 3-4 months at the latest, and very positive effects on the new tissue formation process in the applied areas have been reported[11,12]. It has been proven by characterization studies that naturally obtained DCPD nanoparticles have the potential to be used as an adhesion inhibitor[13,14].

This study aimed to compare the anti-adhesion effects of contractubex (CTX) and dicalcium phosphate dihydrate (DCPD) particles in rats treated with the uterine horn adhesion model, with histological and immunohistochemical tests and biochemical measurements.

Material and methods

Synthesis of nanocrystalline dicalcium phosphate dihydrate from eggshells

The collected white chicken eggshells were washed with distilled water to remove impurity and then boiled in distilled water for 60 min to remove the membrane. Cleaned eggshell materials were dried in the oven at 60°C for 24 h. Afterward, they were manually crushed with agate mortar and pestle and calcined at 900°C for two hours with a heating-cooling rate of 5°C/min. The decomposition of eggshell powder ($CaCO_3$) to CaO occurs according to the equation (1).

$$CaCO_3 \xrightarrow{900°C} CaO + CaO_2 \quad (1)$$

To obtain the purified form of calcium hydroxide Ca(OH)2, CaO were ball milled in the stoichiometric amount of distilled water for 6 h.

Precipitation process

To obtain DCPD crystals was done by direct synthesis in solution. All chemicals were of analytical grade, purchased from Merck, and used as received in the experimental study. A solution (200 mL) containing $Ca(OH)_2$ (0.5 M) and H_3PO_4 (0.3 M) were prepared with the appropriate dilutions. The 0.5 M $Ca(OH)_2$ suspension was vigorously stirred at 70°C for one hour, and the H_3PO_4 (0.3 M) solution was added dropwise and stirred for about 30 min. The pH of the solution was adjusted to 10 by adding 30% NH_3 solution. After the complete edition of the H_3PO_4 solution, an additional vigorous stirring was carried out for one hour at 90°C to activate the chemical reaction. The obtained slurry was left at room temperature overnight for the aging process. During aging at room temperature, the DCPD was precipitated. The excess NH_3 solution obtained over the white precipitate powder was removed, and the precipitate powder was washed several times with distilled water to remove the NH^{4+} ions. The residue was dried at 60°C for 48 h. The chemical reaction between $Ca(OH)_2$ and H_3PO_4 is equation (2)

$$Ca(OH)_2 + H_3PO_4 \rightarrow CaHPO_4.2H_2O \quad (2)$$

Cell culture

In this study, L929 (mouse fibroblast cell line) cells were purchased from American Type Culture Collection. The medium used in our research was DMEM containing 10% fetal bovine serum, 1% L-glutamine, and 1% penicillin-streptomycin. L929 cells were cultured in DMEM in an incubator with 5% CO_2 at 37 ° C.

Cell culture, tissue and organ cultures are used in in-vitro cytotoxicity tests, the most used systems are cell cultures[15]. The use of L929 or Balb/3T3 mouse fibroblast cell line is recommended for the evaluation of cytotoxicity[16,17]. These cells are cell types that can be found easily, reproduce

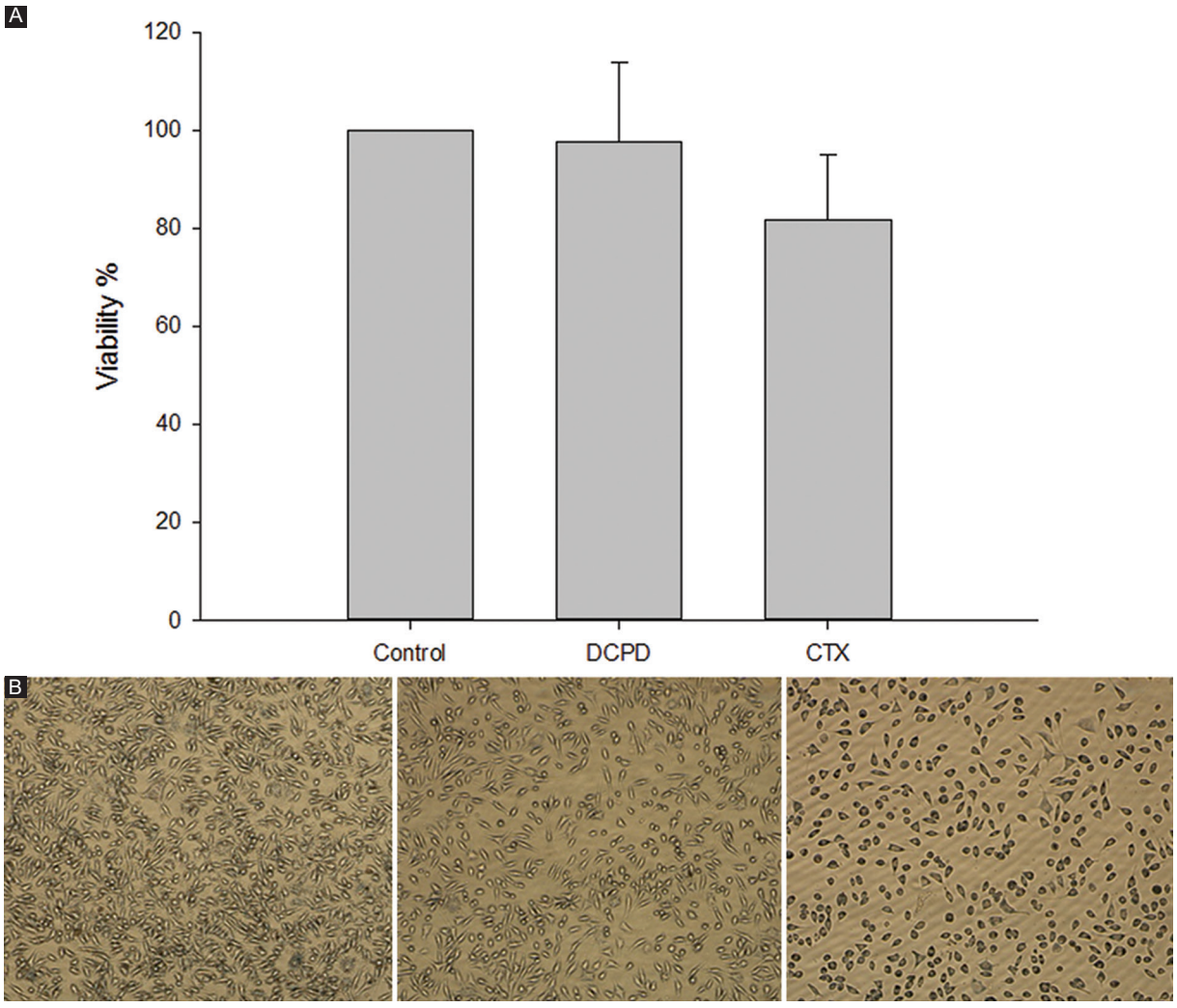

Figure 1. A: *% viability values of DCPD*. **B:** *cell viability of DCPD and CTX in L929 cells. DCPD: dicalcium phosphate dihydrate; CTX: contractubex.*

rapidly and have a homogeneous morphology. With their growth characteristics, they ensure that the experiment can be repeated in cytotoxicity evaluations[18].

The cytotoxicity of DCPD and CTX were compared in the study. In the study performed at different concentrations, it was observed that both substances were not cytotoxic, and DCPD had a more negligible effect on cell viability when counting cells (Fig. 1A and B).

Test animals

In the study, 60 Wistar albino rats, newly adult, 16 weeks old, unmated, female, 200-220 g, were used as experimental animals[3,19,20]. All experimental procedures applied in this study were examined by Sivas Cumhuriyet University Experimental Animal Research Ethics Committee and approved on 25 December 2020 with the number 469. Minimal numbers of animals were used and every efforts were made to minimize their suffering. Wistar albino rats were chosen because of their robustness and low cost compared to large animals[9]. After the rats were purchased, they were kept for one week to acclimate to the laboratory conditions. Rats were kept as two individuals in a cage with standard animal housing conditions in the laboratory, 12 h of light-darkness, 21°C temperature, 50-60% humidity, and standard pellet rat chow and water[3,5,21,22].

Animal model

Experimental groups

G1: Control group, G2: DCPD powder 0.25 g. administration group, G3: DCPD powder 0,5 g. application

group, G4: CTX 1 g application group[23]. A total of 60 rats were randomly divided into four groups. Each group was divided into 7th, 14th, and 21st day groups among themselves. There were 5 rats in subgroups.

The modified rat uterine horn adhesion model to induce intra-abdominal adhesion was chosen because it is a standardized qualitative and quantitative model, mimics reproductive surgery and provides reproducible results and consistent adhesion formation[3,24-26].

All rats have fasted for 12 h before surgery. Anesthesia was administered through intraperitoneal injection of 10 mg/kg xylazine (Rompun; Bayer, Turkey) and 50 mg/kg ketamine (Ketalar; Parke Davis, Turkey, Istanbul), and spontaneous breathing was achieved. All surgical procedures were performed by the same surgeon. The rats were fixed in the supine position; the midline lower abdomen of each rat was shaved and disinfected with iodine solution. The abdomen was entered with a midline vertical incision of approximately 3 cm in length. Five standard lesions were created with 10 W unipolar cautery on the antimesenteric face of the right uterine horns of the rats. The two layers of abdominal wall were closed with 4/0 prolene sutures after the surgery. Second laparotomy was performed in the 7th, 14th and 21st day groups. Intracardiac blood was taken from the animals according to the groups, and the animals were euthanized by the neck dislocation method.

Adhesion scoring

Adhesions formed after laparotomy was evaluated macroscopically by two independent researchers unaware of the applications. The mean score of both researchers was used for that rat. Grading of adhesions was evaluated in terms of adhesion prevalence and severity, with scores from 0 to 4[27]. Adhesion prevalence and severity scores for each rat were added to give the respective rat's total adhesion score.

Biochemical examination

After the animals were sacrificed, 5cc of blood was taken into a tube with EDTA by intracardiac route[28,29]. The collected blood was centrifuged at 3000 rpm for 15 minutes and then separated into the serum. Tumor necrosis factor (TNF)-α (Cat No: E0764Ra) and interleukin (IL)-1 (Cat No: E010Ra) from cytokines and vascular endothelial growth factor (VEGF, Cat No: E065Ra) from the growth factor were studied in serum samples taken following the guide of the kit for the enzyme-linked immunosorbent assay (ELISA) method.

Histopathological studies

Uterine horns were removed from sacrificed rats and fixed in 10% neutral buffered formalin for 48 hours for histological examination. Tissues washed in tap water were embedded in paraffin blocks after tissue follow-up processes according to standard protocol. 3-5 μm sections were taken from paraffin blocks, and routine hematoxylin-eosin (H&E) staining was performed to evaluate the layers of the organ and the healing rates in the wound.

For immunohistochemical evaluation, tissue blocks were re-sectioned, deparaffinized, passed through a decreasing series of ethyl alcohol (100-90-96-80-70%), and washed in buffered phosphate solution (PBS) for 5 min. At the end of the period, the sections were boiled in buffered citrate at pH 6 for 20 min in the microwave for antigen retrieval. Sections cooled at room temperature were washed in PBS for 5 min and kept in a 3% hydrogen peroxide (H2O2) solution prepared with distilled water for 10 min to suppress endogenous peroxidase activity. At the end of the time, the sections were washed with PBS for 3 × 5 min and then kept at room temperature for 20 min by dripping ultra V block (Thermo Scientific, USA) to prevent non-specific binding. With the help of blotting paper, the block solution was removed without washing, and the primary antibodies VEGF (monoclonal antibody, JH121, ThermoFisher, USA) and TGF-β1 (ThermoFisher, USA) were kept in a humid and dark environment for 1.5 h at 36°C.

After the primary antibody application, the sections were washed with PBS for 3 × 5 min, and the first Biotinylated Goat Anti Polyvalent was dripped, washed with PBS, then Streptavidin peroxidase (Thermo Scientific, USA) was dropped and kept in a humid and dark environment at 36°C for 20 min. At the end of the time, the sections were washed with PBS, and chromogen (Thermo Scientific, USA) was dripped onto 3,3'Diaminobenzidine (DAB) and waited for 5 min. Colored sections were washed with PBS, treated with Mayer's hematoxylin for 1 min, ground dyed, rewashed, covered with a particular concealer, examined under a microscope, and photographed (Olympus BX51, Japan)[30].

Statistical analyzes

The mean (standard deviation/standard error) or median (25-75% interquartile range) of the data were

calculated. In the analysis of the data, correlational tests such as ANOVA or Kruskal–Wallis (followed by post hoc tests such as Tukey or Mann–Whitney when significant) and correlation tests were used. A $p < 0.05$ was considered statistically significant. The sample size for each group was calculated with the online program "StatsToDo: Sample Size for Measurement Differences Between Unpaired Groups" module. (http://www.statstodo.com/SSizUnpairedDiff_Pgm.php) power was taken as 80% (1-b = 0.80) and 5% significance level (a < 0.05) with the desired statistical data.

Results

Adhesion scoring

Adhesion was observed most in G1. The results of G3 and G4 were similar but less than G2 (Table 1). It was observed that the amount of adhesion decreased as the DCPD dose increased, and the amount of adhesion was the least compared to the CTX group when high doses were used. It was determined that adhesion decreased within days in both CTX and DCPD groups (Table 2).

Table 1. Adhesion scoring

Total adhesion score	7th day	14th day	21st day
G1	7, 8, 8, 7, 8	6, 7, 7, 6, 7	6, 7, 7, 5, 6
G2	6, 6, 5, 5, 5	5, 5, 4, 3, 3	5, 4, 4, 3, 3
G3	3, 3, 3, 3, 2	3, 2, 3, 3, 2	2, 2, 2, 2, 2
G4	5, 5, 4, 4, 3	5, 5, 4, 3, 3	4, 4, 3, 3, 3

Table 2. Adhesion score statistics

Groups	Adhesion			p
	7th day	14th day	21st day	
G1	8 ± 1	7 ± 1	6 ± 1	*0.010*[a]
G2	5 ± 1	4 ± 2	4 ± 1	*0.009*[b]
G3	3 ± 0	3 ± 1	2 ± 0	*0.039*[c]
G4	4 ± 1	4 ± 2	3 ± 1	*0.039*[d]
p	*0.001*[e]	*0.002*[f]	*0.001*[g]	

In italics: statistically significant.
[a] $p_{7\ day\text{-}14\ day} = 0.025$; $p_{7\ day\text{-}21\ day} = 0.038$.
[b] $p_{7\ day\text{-}14\ day} = 0.038$; $p_{7\ day\text{-}21\ day} = 0.038$.
[c] $p_{7\ day\text{-}21\ day} = 0.046$.
[d] $p_{7\ day\text{-}21\ day} = 0.046$.
[e] $p_{G1\text{-}G2} = 0.007$; $p_{G1\text{-}G3} = 0.006$; $p_{G1\text{-}G4} = 0.008$; $p_{G2\text{-}G3} = 0.006$; $p_{G2\text{-}G4} = 0.033$; $p_{G3\text{-}G4} = 0.018$.
[f] $p_{G1\text{-}G2} = 0.008$; $p_{G1\text{-}G3} = 0.007$; $p_{G1\text{-}G4} = 0.008$; $p_{G2\text{-}G3} = 0.033$; $p_{G3\text{-}G4} = 0.033$.
[g] $p_{G1\text{-}G2} = 0.011$; $p_{G1\text{-}G3} = 0.005$; $p_{G1\text{-}G4} = 0.008$; $p_{G2\text{-}G3} = 0.005$; $p_{G3\text{-}G4} = 0.005$.

Biochemical examination

TNF-alpha, IL-1β, and VEGF levels in intracardiac blood taken from animals were measured by the ELISA method.

TNF-α was found in G1 at 121.8889 ng/mL ± 13.7400 on day 7, 77.4444 ng/mL ± 15.7300 on day 14, and 60.7778 ng/mL ± 15.9300 on day 21. In G3, it was found 93.0000 ng/mL ± 10.4626 on day 7, 68.0741 ng/mL ± 20.0890 on day 14, and 53.3704 ng/mL ± 11.4156 on day 21. While the amount of TNF-α decreased as the number of days increased within the groups, the amount of TNF-α decreased more in G2 and G3 compared to G1 (Fig. 2A).

IL-1β was found in G1 to be 22.5397 ng/mL ± 0.8900 at day 7, 20.1587 ng/mL ± 0.8600 at day 14, and 14.9206 ng/mL ± 0.5590 at day 21, while G3 It was found to be 15.7143 ng/mL ± 0.7800 on day 7, 11.9841 ng/mL ± 0.6500 on day 14, and 11.9048 ng/mL ± 0.7400 on day 21. While the amount of IL-1β decreased as the number of days increased within the groups, the amount of IL-1β decreased even more in G3 compared to the control group (Fig. 2B).

VEGF was found to be 454.000 ng/mL ± 10.6483 on day 7, 334.6667 ng/mL ± 15.7380 on day 14, and 270.0000 ng/mL ± 12.8469 on day 21 in G1. In G3, it was found to be 298.6667 ng/mL ± 32.0740 on the 7th day, 242.0000 ng/mL ± 19.6186 on the 14th day, and 107.3333 ng/mL ± 31.6287 on the 21st day. The amount of VEGF decreased with days in G2 and G3 more than the other groups (Fig. 2C).

Histopathological evaluation

For general light microscope evaluation, H&E staining and post-incision healing sites were evaluated for the integrity of the uterine layers and inflammatory cell density. G2 and G3 recovered faster than G4. The integrity of the tissue layer was quickly preserved, with less inflammatory cell density in G3 than G4 in the healing areas. In G4, inflammatory cells were less than in the control group but more than in the experimental groups (Fig. 3).

Immunohistochemical localization evaluation was made by including the perimetrium layer, the adjacent border of the uterus with the peritoneum. Accordingly, TGF-β1 and VEGF localization gradually increased in

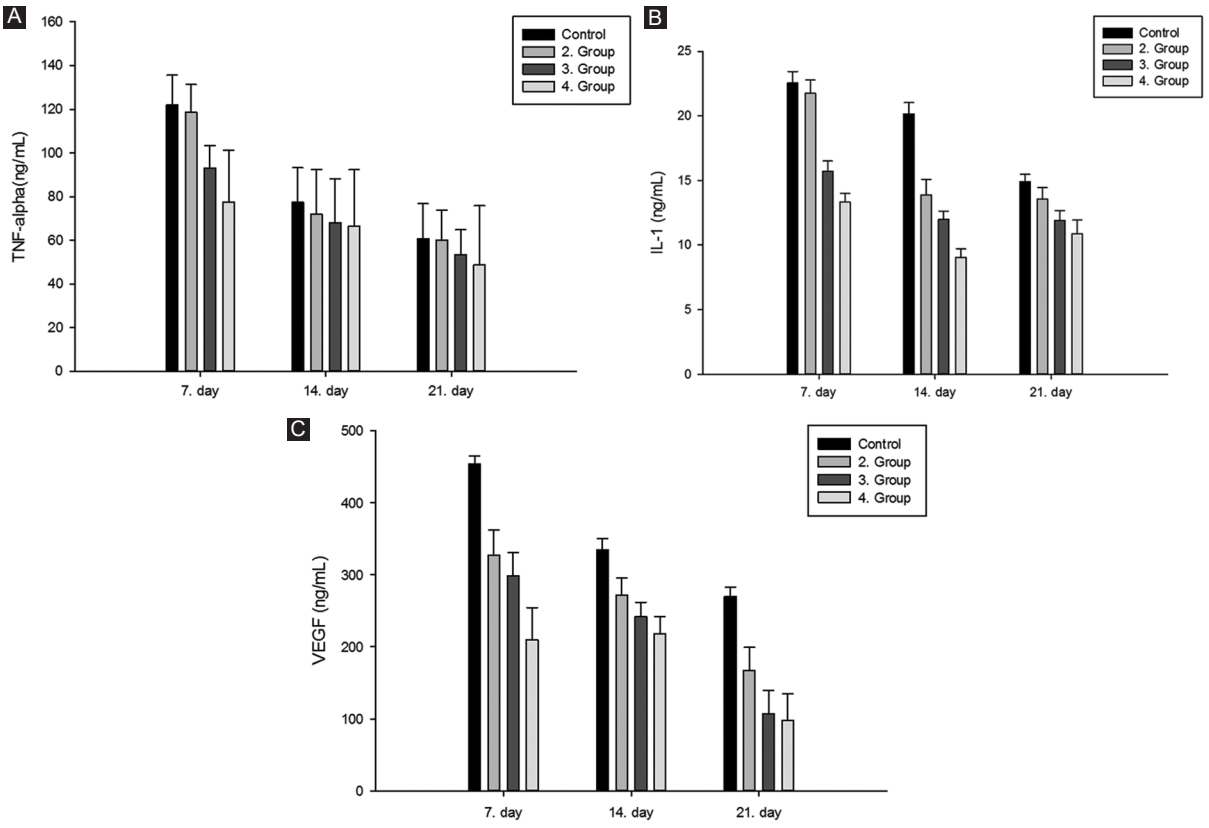

Figure 2. A: *amounts of TNF-α on days 7, 14 and 21 between groups.* **B:** *amounts of IL-1β between the groups on days 7, 14 and 21.* **C:** *VEGF amounts on days 7, 14 and 21 between groups. TNF-α: tumor necrosis factor alpha; IL-1β: interleukin-1β; VEGF: vascular endothelial growth factor.*

G1 on the 7th, 14th, and 21st days, and it was evaluated as having the highest localization degree when compared to all groups (Tables 3 and 4).

Although TGF-β1 and VEGF localization were less in the G2 group compared to G1, the least TGF-β1 and VEGF immunolocalization were detected in the G3 and G4 groups. For both antibodies, the least localization among all groups belonged to G3. The highest TGF-β1 immunolocalization was observed from day 7 to day 21 in G1, with less localization in G2 and lowest localization in G3 (Fig. 4).

When TGF-β1 immune localization score statistics were compared, on the 14th day, the TGF-β1 level was found to be higher between G1 and G3. When G1 and G4 were compared, it was observed that the TGF-β1 level in G1 was higher. TGF-β1 level was higher in G2 than in G3 (Table 3). As DCPD dose increased in G2 and G3, TGF level decreased and the highest decrease was observed in G4 (Table 5).

The highest VEGF immune localization was observed in G1 from day 7 to day 21, with lesser localization in G2 and the lowest localization in G3 (Fig. 5).

As the number of days increased, while the most VEGF immune localization score statistics were in G1 and G2, it was found at least in G3 (Table 6).

Discussion

Intra-abdominal adhesions resulting from a surgical procedure can cause complications even decades later. Patient symptoms include chronic abdominal pain, infertility, and intestinal obstruction and often cannot be attributed to their cause. Chronic lower abdominal pain severely impairs the quality of life of those affected and is an indication for 30-50% of all laparoscopies and 5% of hysterectomies[31]. With a better understanding of the morbidity and mortality associated with pelvic adhesions, the development of models to help prevent adhesions remains an important research topic. In this context, researches are carried out in which the anti-adhesive properties of various agents applied as nanoparticles are also tested[1,2,5]. Anti-adhesion prophylactic agents should provide an anti-adhesive action that is highly biocompatible and absorbable, protecting

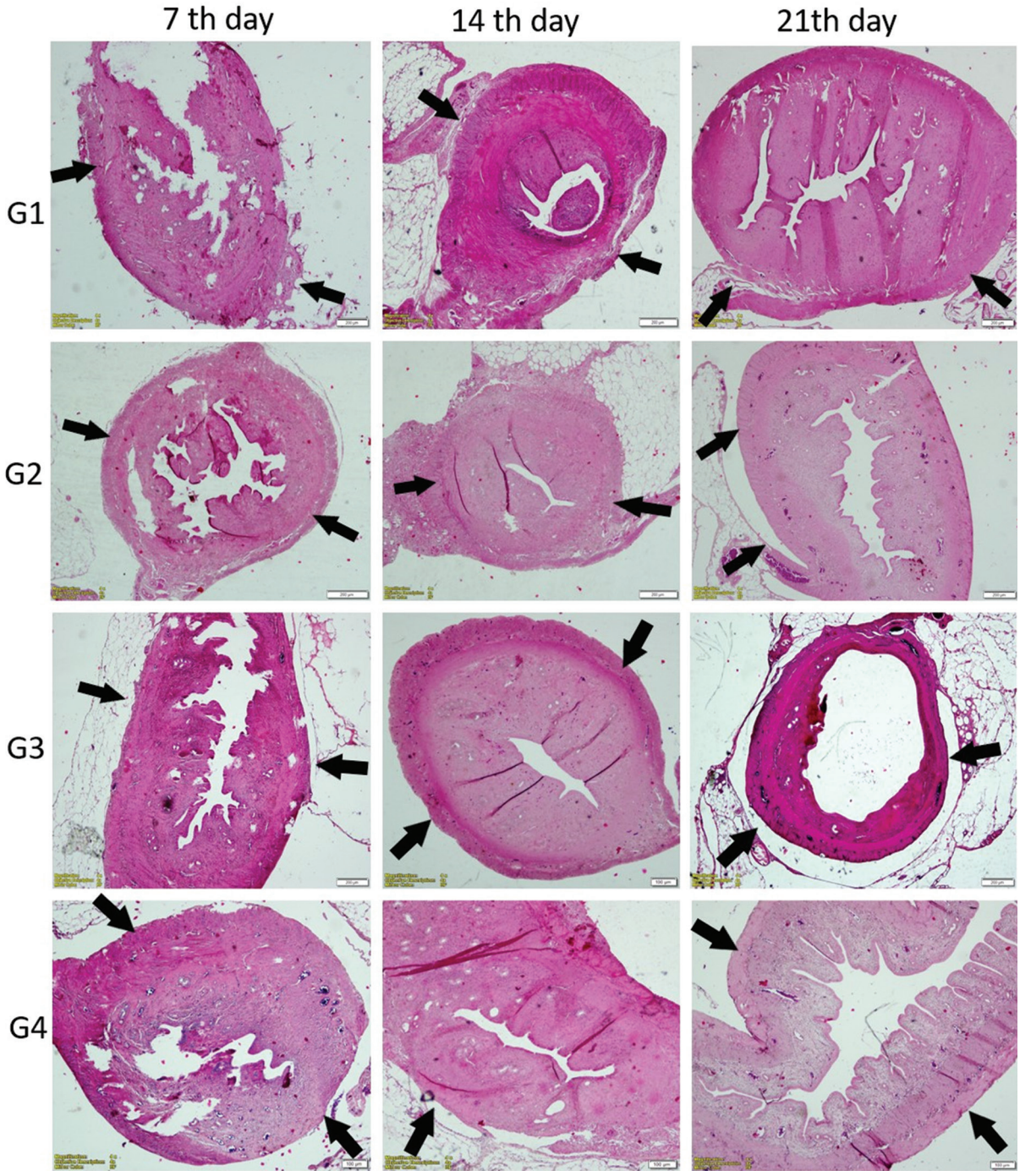

Figure 3. *In the G1, G2, G3, G4 groups, the general histological image of the adhesion areas of the uterus with the perimetrium layer on days 7, 14 and 21, and the incision area in the perimetrium layer are marked with a black arrow (H&E staining, ×10 magnification). Due to the rapid recovery, especially in G3, the uterine tissue layers were observed more regularly.*

against new and recurrent adhesions, tissue separation, and protection of peritoneal surfaces. Low cost is also of great importance. In our study, we compared the anti-adhesion effect of DCPD nanoparticles with CTX with proven effectiveness.

Postoperative adhesion formation involves three basic processes: 1. inhibition of fibrinolytic and extracellular matrix degradation systems, 2. induction of cytokines production and an inflammatory response involving TGF-β, and 3. induction of tissue hypoxia

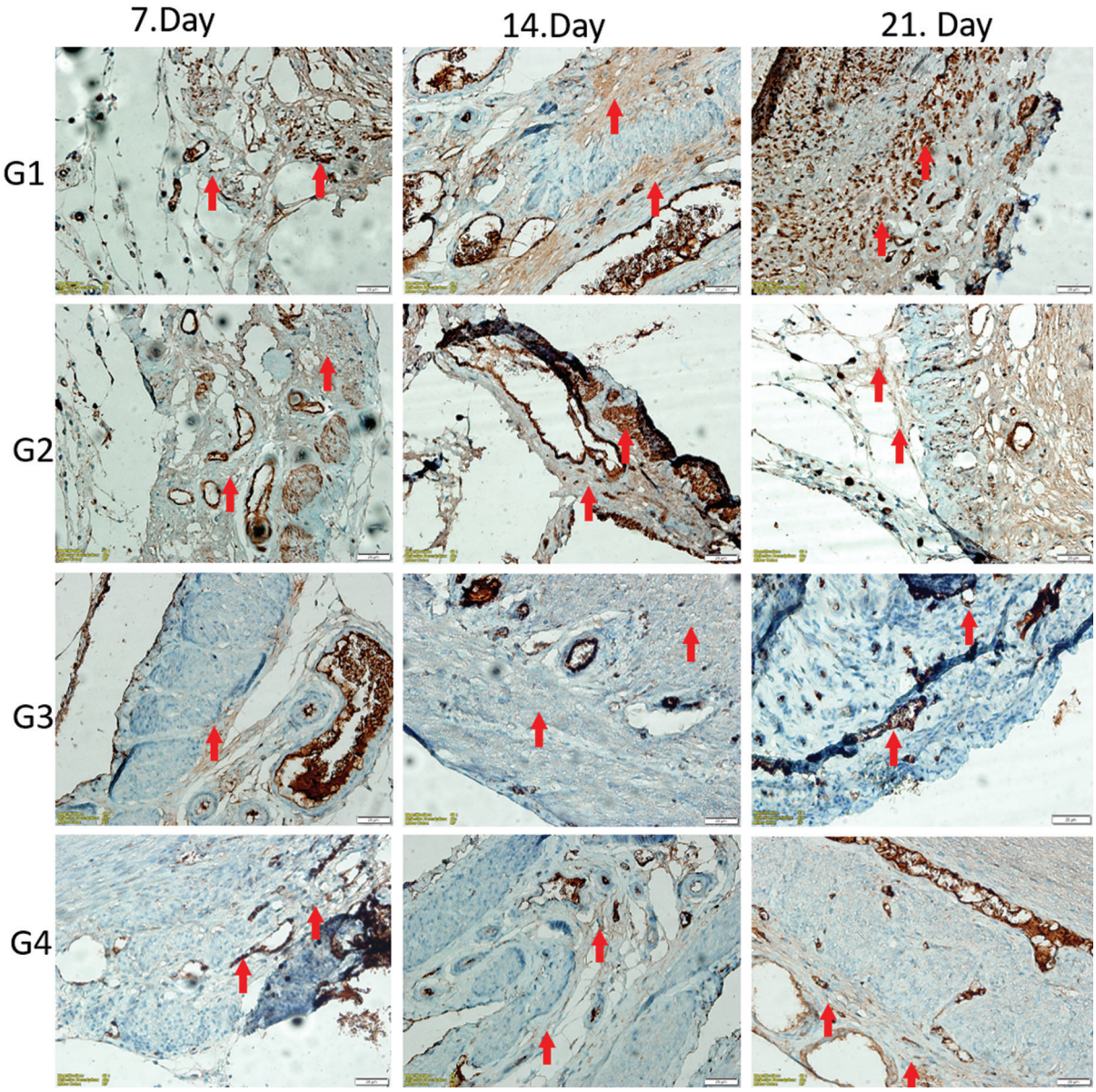

Figure 4. *In G1, G2, G3, G4 groups, brown areas showing TGF-β1 immune localization on the 7th, 14th and 21st days of the uterine perimetrium layer and adhesion areas are observed with a red arrow (TGF-β1 antibody, ×40 magnification). It was determined that the highest TGF-β1 immunolocalization was in G1 from day 7 to day 21, lesser localization in G2 and the least localization in G3. TGF-β1: transforming growth factor-beta 1.*

leading to increased expression of VEGF[1,32]. Changes in cytokine levels TGF-β and VEGF are critical molecules in pathological tissue fibrosis. TGF β1 has a well-defined role in cell differentiation, angiogenesis, and fibroblast activation. It has been suggested to be the major profibrotic mediator of the process[33]. As the number of days increased, the lowest localization among all groups was seen in G3 for both antibodies. This finding was similar to the adhesion level detected in all groups. The amount of adhesion developed the most in G1 and G2, and the least in the group G3 and G4. In addition, in the histopathological evaluation of our study G2 and G3 recovered faster than G4. The integrity of the tissue layer was rapidly preserved, and less inflammatory cell density was determined in G3 than G2 in the healing areas. In G4, inflammatory cells were found to be less than in the G1, but more than in G2 and G3.

In the biochemical evaluation, it was determined that the highest decrease in VEGF level was observed

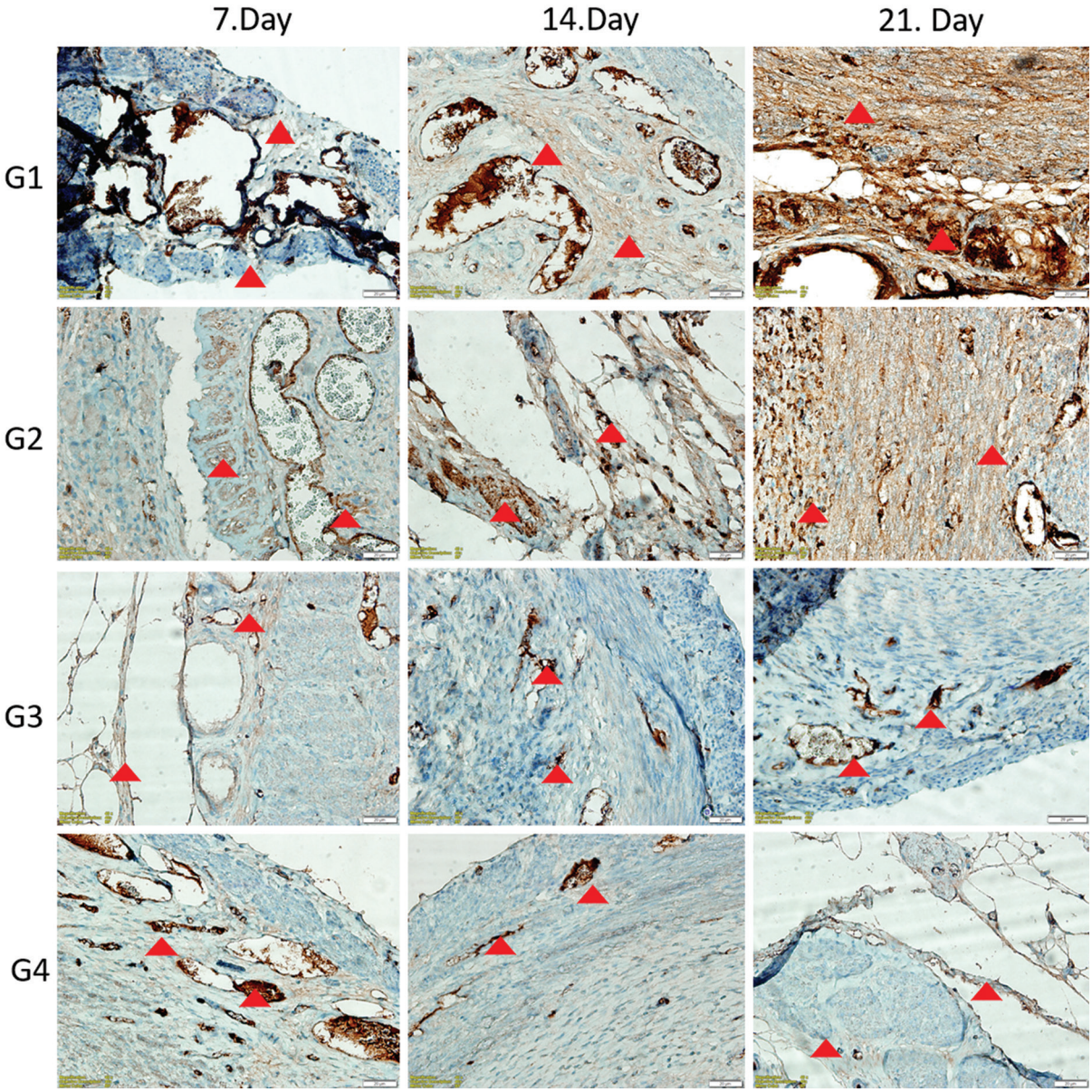

Figure 5. *In G1, G2, G3, G4 groups, brown areas showing VEGF immune localization on the 7th, 14th and 21st days of the uterine perimetrium and adhesion areas are observed with a red triangle (VEGF antibody, ×40 magnification). It was determined that the highest VEGF immunolocalization was in G1 from day 7 to day 21, lesser localization in G2 and the least localization in G3. VEGF: vascular endothelial growth factor.*

Table 3. TGF-β1 immune localization scoring

TGF-β1	7th day	14th day	21st day
G1	1, 1, 1, 1, 2	2, 2, 1, 1, 1	2, 3, 2, 2, 1
G2	1, 2, 1, 1, 2	2, 3, 3, 2, 3	3, 3, 3, 4, 4
G3	2, 2, 2, 2, 1	2, 4, 4, 4, 3	4, 4, 4, 3, 4
G4	1, 1, 3, 2, 2,	2, 3, 3, 3, 3, 1	2, 3, 3, 3, 3

TGF-β1: Transforming growth factor-β 1.

in G4, followed by G3 and G2, respectively. In G3 IL-1 levels showed a significant decrease after the 14th day. TNF-α can promote interleukin production from mesenchymal cells. High TNF-α levels in peritoneal fluid and serum correlate with adhesion severity[34]. In our study, it was observed that TNF-α levels decreased as the number of days increased. The decrease in TNF-α levels was greater in G3 than in G1 and G2.

Table 4. VEGF immune localization scoring

VEGF	7th day	14th day	21st day
G1	1, 1, 1, 1, 2	3, 2, 1, 1, 1	2, 2, 1, 1, 1
G2	1, 2, 1, 1, 2	2, 3, 3, 2, 3	2, 3, 2, 2, 2
G3	2, 2, 2, 2, 1	4, 4, 4, 4, 3	2, 3, 3, 3, 4
G4	1, 1, 3, 2, 2,	2, 2, 2, 2, 3	2, 2, 1, 3, 3

VEGF: Vascular endothelial growth factor.

Table 5. TGF immune localization score statistics

Groups	TGF			p
	7th day	14th day	21st day	
G1	3 ± 0	4 ± 1	5 ± 0	*0.010*[a]
G2	3 ± 1	3 ± 0	4 ± 1	0.097
G3	2 ± 1	2 ± 1	1 ± 0	0.368
G4	2 ± 0	2 ± 0	2 ± 1	0.584
p	0.081	*0.005*[b]	*0.001*[c]	

In italics: statistically significant.
[a]$p_{7\ day\text{-}21\ day} = 0.041$; $p_{14\ day\text{-}21\ day} = 0.034$.
[b]$p_{G1\text{-}G3} = 0.007$; $p_{G1\text{-}G4} = 0, 013$; $p_{G2\text{-}G3} = 0.016$.
[c]$p_{G1\text{-}G2} = 0.016$; $p_{G1\text{-}G3} = 0.005$; $p_{G1\text{-}G4} = 0.006$; $p_{G2\text{-}G3} = 0.006$; $p_{G2\text{-}G4} = 0.007$.
TGF: transforming growth factor.

Table 6. VEGF immune localization score statistics

Groups	VEGF			p
	7th day	14th day	21st day	
G1	3 ± 1	3 ± 1	4 ± 1	*0.014*[a]
G2	2 ± 1	3 ± 2	4 ± 1	*0.024*[b]
G3	2 ± 0	2 ± 0	1 ± 1	0.174
G4	2 ± 0	2 ± 0	2 ± 0	0.926
p	0.365	*0.014*[c]	*0.001*[d]	

In italics: statistically significant.
[a]$p_{7\ day\text{-}14\ day} = 0.046$; $p_{7\ day\text{-}21\ day} = 0.041$.
[b]$p_{7\ day\text{-}21\ day} = 0.041$.
[c]$p_{G1\text{-}G3} = 0.006$; $p_{G1\text{-}G4} = 0.016$; $p_{G2\text{-}G3} = 0.045$.
[d]$p_{G1\text{-}G3} = 0.007$; $p_{G1\text{-}G4} = 0.006$; $p_{G2\text{-}G3} = 0.008$; $p_{G2\text{-}G4} = 0.007$.
VEGF: vascular endothelial growth factor.

Conclusion

These experimental results show that DCPD nanoparticles show promise as a clinical antiadhesive agent and should be further evaluated in experimental animal models and human trials. DCPD nanoparticles are easy to administer and cost advantageous, and could be helpful in surgical practice if their efficacy is confirmed in clinical trials. It appears valuable and safe for clinical practice and prevents adhesion formation after abdominal surgery.

Funding

This study was supported by Sivas Cumhuriyet University Scientific Research Projects (CUBAP) with project number 2021 T-910.

Conflicts of interest

Authors declare no conflicts of interest for this article.

Ethical disclosures

Protection of human and animal subjects. The authors declare that the procedures followed were in accordance with the regulations of the relevant clinical research ethics committee and with those of the Code of Ethics of the World Medical Association (Declaration of Helsinki).

Confidentiality of data. The authors declare that no patient data appear in this article.

Right to privacy and informed consent. The authors declare that no patient data appear in this article.

References

1. Hassanabad AF, Zarzycki AN, Jeon K, Dundas JA, Vasanthan V, Deniset JF, et al. Prevention of post-operative adhesions: a comprehensive review of present and emerging strategies. Biomolecules. 2021;11:1027.
2. Park H, Baek S, Kang H, Lee D. Biomaterials to prevent post-operative adhesion. Materials (Basel, Switzerland). 2020;13:3056.
3. Wallwiener M, Yvonne BS, Hierlemann H, Brochhausen C, Solomayer E, Wallwiener C. Innovative barriers for peritoneal adhesion prevention: liquid or solid? A rat uterine horn model. Fertil Steril. 2006;86:1266-76.
4. Çakir C, Okuyan E, Tokgöz B, Karakoc G, Ozkaya E, Kucukozkan T. Effects of heparin and prednisolone on postoperative intra-abdominal adhesions in Wistar rats. J Surg Med. 2020;4:447-50.
5. Yan S, Yue Y, Zeng L, Yue J, Li WL, Mao CQ, et al. Effect of intra-abdominal administration of ligustrazine nanoparticles nano spray on postoperative peritoneal adhesion in rat model. J Obstet Gynaecol Res. 2015;41:1942-50.
6. Esposito AJ, Heydrick SJ, Cassidy MR, Gallant J, Stucchi AF, Becker JM. Substance P is an early mediator of peritoneal fibrinolytic pathway genes and promotes intra-abdominal adhesion formation. J Surg Res. 2013;181:25-31.
7. Beuth J, Hunzelmann N, Van Leendert R, Basten R, Noehle M, Schneider B. Safety and efficacy of local administration of contractubex to hypertrophic scars in comparison to corticosteroid treatment. Results of a multicenter, comparative epidemiological cohort study in Germany. *In Vivo*. 2006;20:277-83.
8. Fischer S, Ernst HR, Drücke D, Diehm Y, Lehnhardt M, Daigeler A. Topical preparations for prevention and treatment of hypertrophic scars and keloids: a literature review. Handchir Mikrochir Plast Chir. 2015; 47:253-67.
9. Allègre L, Le Teuff I, Leprince S, Warembourg S, Taillades H, Garric X, et al. A new bioabsorbable polymer film to prevent peritoneal adhesions validated in a post-surgical animal model. PLoS One. 2018;13:e0202285.
10. Seref K, Sonmez K, Gulburun MA, Ekinci O, Oge CB, Gulbahar O, et al. Protective effects of contractubex® on stricture formation after experimental corrosive esophageal burns in rats. Arch Med Res. 2020;51:664-9.

11. Pina S, Vieira SI, Rego P, Torres PM, da Cruz e Silva OA, da Cruz e Silva EF, et al. Biological responses of brushite-forming Zn-and ZnSr-substituted beta-tricalcium phosphate bone cements. Eur Cells Mater. 2010;20:162-77.
12. Theiss F, Apelt D, Brand B. Biocompatibility and resorption of a brushite calcium phosphate cement. Biomaterials. 2005;26:4383-94.
13. Vahabzadeh S, Bandyopadhyay A, Bose S, Mandal R, Nandi SK. IGF-loaded silicon and zinc doped brushite cement: physico-mechanical characterization and *in vivo* osteogenesis evaluation. Integr Biol (Camb). 2015;7:1561-73.
14. Roy M, DeVoe K, Bandyopadhyay A, Bose S. Mechanical property and *in vitro* biocompatibility of brushite cement modified by polyethylene glycol. Mater Sci Eng C Mater Biol Appl. 2012;32:2145-52.
15. Schmalz G. Use of cell cultures for toxicity testing of dental materials--advantages and limitations. J Dent. 1994;22 Suppl 2:S6-11.
16. Thonemann B, Schmalz G, Hiller KA, Schweikl H. Responses of L929 mouse fibroblasts, primary and immortalized bovine dental papilla-derived cell lines to dental resin components. Dent Mater. 2002;18:318-23.
17. Bouillaguet S, Shaw L, Gonzalez L, Wataha JC, Krejci I. Long-term cytotoxicity of resin-based dental restorative materials. J Oral Rehabil. 2002;29:7-13.
18. Cao T, Saw TY, Heng BC, Liu H, Yap AU, Ng ML. Comparison of different test models for the assessment of cytotoxicity of composite resins. J Appl Toxicol. 2005;25:101-8.
19. Akdemir A, Sahin C, Erbas O, Yeniel AO, Sendag F. Is ursodeoxycholic acid crucial for ischemia/reperfusion-induced ovarian injury in rat ovary? Arch Gynecol Obstet. 2015;292:445-50.
20. Gungor AN, Gencer M, Karaca T, Hacivelioglu S, Uysal A, Korkmaz F, et al. The effect of hesperetin on ischemia-reperfusion injury in rat ovary. Arch Gynecol Obstet. 2014;290:763-9.
21. Guo J, Wang Y, Wang N, Bai Y, Shi D. Celastrol attenuates intrahepatic cholestasis of pregnancy by inhibiting matrix metalloproteinases-2 and 9. Ann Hepatol. 2019;18:40-7.
22. Muglali M, Yılmaz N, Inal S, Guvenc T. Immunohistochemical comparison of indermil with traditional suture materials in dental surgery. J Craniofac Surg. 2011;22:1875-9.
23. Aysan E, Bektas H, Ersoz F, Sari S, Huq G. Effects of contractubex on the prevention of postoperative peritoneal adhesion. J Surg Res. 2010;164:193-7.
24. Bakkum EA, van Blitterswijk CA, Dalmeijer RA, Trimbos JB. A semiquantitative rat model for intraperitoneal postoperative adhesion formation. Gynecol Obstet Invest. 1994;37:99-105.
25. Hill-West JL, Chowdhury SM, Dunn RC, Hubbell JA. Efficacy of a resorbable hydrogel barrier, oxidized regenerated cellulose, and hyaluronic acid in the prevention of ovarian adhesions in a rabbit model. Fertil Steril. 1994;62:630-4.
26. Szabo A, Haj M, Waxsman I, Eitan A. Evaluation of seprafilm and amniotic membrane as adhesion prophylaxis in mesh repair of abdominal wall hernia in rats. Eur Surg Res. 2000;32:125-8.
27. Linsky CB, Diamond MP, Cunningham T, Constantine B, DeCherney AH, diZerega GS. Adhesion reduction in the rabbit uterine horn model using an absorbable barrier, TC-7. J Reprod Med. 1987;32:17-20.
28. Demir M, Yilmaz B, Kalyoncu S, Tuncer M, Bozdag Z, Ince O, et al. Metformin reduces ovarian ischemia reperfusion injury in rats by improving oxidative/nitrosative stress. Taiwan J Obstet Gynecol. 2021;60:45-50.
29. Melekoglu R, Ciftci O, Eraslan S, Alan S, Basak N. The protective effects of glycyrrhetinic acid and chrysin against ischemia-reperfusion injury in rat ovaries. BioMed Res Int. 2018;2018:5421308.
30. Fedchenko N, Reifenrath J. Different approaches for interpretation and reporting of immunohistochemistry analysis results in the bone tissue-a review. Diagn Pathol. 2014;9:221.
31. Kaya F, Kismet K, Ozer H, Soylu VG, Duymus ME, Akgun YA, et al. Can platelet-rich plasma be used safely in intra-abdominal operations? Bratisl Lek Listy. 2016;117:525-9.
32. Coccolini F, Ansaloni L, Manfredi, Campanati L, Poiasina E, Bertoli P, et al. Peritoneal adhesion index (PAI): proposal of a score for the "ignored iceberg" of medicine and surgery. World J Emerg Surg. 2013;8:6.
33. Chegini N. TGF-β system: the principal profibrotic mediator of peritoneal adhesion formation. Semin Reprod Med. 2008;26:298-312.
34. Kaidi AA, Gurchumelidze T, Nazzal M, Figert P, Vanterpool C, Silva Y. Tumor necrosis factor-α: a marker for peritoneal adhesion formation. J Surg Res. 1995;58:516-8.